3

Direct and Inverse Heat Transfer Problems in Dynamics of Plate Fin and Tube Heat Exchangers

Dawid Taler
University of Science and Technology, Cracow
Poland

1. Introduction

Plate fin and tube heat exchangers can be manufactured from bare or individual finned tubes or from tubes with plate fins. Tubes can be circular, oval, rectangular or other shapes (Hesselgreaves, 2001; Kraus et al., 2001). The mathematical models of the heat exchanger were built on the basis of the principles of conservation of mass, momentum and energy, which were applied to the flow of fluids in the heat exchangers. The system of differential equations for the transient temperature of the both fluids and the tube wall was derived. Great emphasis was put on modelling of transient tube wall temperatures in thin and thick walled bare tubes and in individually finned tubes. Plate - fin and tube heat exchangers with oval tubes were also considered.

The general principles of mathematical modeling of transient heat transfer in cross-flow tube heat exchangers with complex flow arrangements which allow the simulation of multipass heat exchangers with many tube rows are presented.

At first, a mathematical model of the cross-flow plate-fin and tube heat exchanger with one row of tubes was developed. A set of partial nonlinear differential equations for the temperature of the both fluids and the wall, together with two boundary conditions for the fluids and initial boundary conditions for the fluids and the wall, were solved using Laplace Transforms and an explicit finite-difference method. The comparison of time variations of fluid and tube wall temperatures obtained by analytical and numerical solutions for step-wise water or air temperature increase at the heat exchanger inlets proves the numerical model of the heat exchanger is very accurate.

Based on the general rules, a mathematical model of the plate-fin and tube heat exchanger with the complex flow arrangement was developed. The analyzed heat exchanger has two passes with two tube rows in each pass. The number of tubes in the passes is different. In order to study the performance of plate-fin and tube heat exchangers under steady-state and transient conditions, and to validate the mathematical model of the heat exchanger, a test facility was built. The experimental set-up is an open wind tunnel.

First, tests for various air velocities and water volumetric flow rates were conducted at steady-state conditions to determine correlations for the air and water-side Nusselt numbers using the proposed method based on the weighted least squares method. Transient

experimental tests were carried out for sudden time changes of air velocity and water volumetric flow rate before the heat exchanger. The results obtained by numerical simulation using the developed mathematical model of the investigated heat exchanger were compared with the experimental data. The agreement between the numerical and experimental results is very satisfactory.
Then, a transient inverse heat transfer problem encountered in control of fluid temperature in heat exchangers was solved. The objective of the process control is to adjust the speed of fan rotation, measured in number of fan revolutions per minute, so that the water temperature at the heat exchanger outlet is equal to a time-dependant target value. The least squares method in conjunction with the first order regularization method was used for sequential determining the number of revolutions per minute. Future time steps were used to stabilize the inverse problem for small time steps. The transient temperature of the water at the outlet of the heat exchanger was calculated at every iteration step using a numerical mathematical model of the heat exchanger. The technique developed in the paper was validated by comparing the calculated and measured number of the fan revolutions. The discrepancies between the calculated and measured revolution numbers are small.

2. Dynamics of a cross-flow tube heat exchanger

Applications of cross-flow tubular heat exchangers are condensers and evaporators in air conditioners and heat pumps as well as air heaters in heating systems. They are also applied as water coolers in so called 'dry' water cooling systems of power plants, as well as in car radiators. There are analytical and numerical mathematical models of the cross-flow tube heat exchangers which enable to determine the steady state temperature distribution of fluids and the rate of heat transferred between fluids (Taler, 2002; Taler & Cebula, 2004; Taler, 2004). In view of the wide range of applications in practice, these heat exchangers were experimentally examined in steady-state conditions, mostly to determine the overall heat transfer coefficient or the correlation for the heat transfer coefficients on the air side and on the internal surface of the tubes (Taler, 2004; Wang, 2000). There exist many references on the transient response of heat exchangers. Most of them, however, focus on the unsteady-state heat transfer processes in parallel and counter flow heat exchangers (Tan, 1984; Li, 1986; Smith, 1997; Roetzel, 1998). In recent years, transient direct and inverse heat transfer problems in cross-flow tube heat exchangers have also been considered (Taler, 2006a; Taler, 2008; Taler, 2009). In this paper, the new equation set describing transient heat transfer process in tube and fin cross-flow tube exchanger is given and subsequently solved using the finite difference method (finite volume method). In order to assess the accuracy of the numerical solution, the differential equations are solved using the Laplace transform assuming constant thermo-physical properties of fluids and constant heat transfer coefficients. Then, the distributions of temperature of the fluids in time and along the length of the exchanger, found by both of the described methods, are compared. In order to assess the accuracy of the numerical model of the heat exchanger, a simulation by the finite difference method is validated by a comparison of the obtained temperature histories with the experimental results. The solutions presented in the paper can be used to analyze the operation of exchangers in transient conditions and can find application in systems of automatic control or in the operation of heat exchangers.

2.1 Mathematical model of one-row heat exchanger

A mathematical model of the cross flow tubular heat exchanger, in which air flows transversally through a row of tubes (Fig. 1), will be presented. The system of partial differential equations describing the space and time changes of: water T_1, tube wall T_w , and air T_2 temperatures are, respectively

$$\frac{1}{N_1}\frac{\partial T_1}{\partial x^+}+\tau_1\frac{\partial T_1}{\partial t}=-\left(T_1-T_w\right), \tag{1}$$

$$\tau_w\frac{\partial T_w}{\partial t}+\tau_f\frac{\partial T_{m2}}{\partial t}+T_w=\frac{h_1U_w}{h_1U_w+h_oU_z}T_1+\frac{h_oU_z}{h_1U_w+h_oU_z}T_{m2}, \tag{2}$$

$$\frac{1}{N_2}\frac{\partial T_2}{\partial y^+}+\tau_2\frac{\partial T_2}{\partial t}=T_w-T_2, \tag{3}$$

where T_{m2} denotes the mean air temperature over the row thickness, defined as

$$T_{m2}=\int_0^1 T_2\left(x^+,y^+,t\right)dy^+. \tag{4}$$

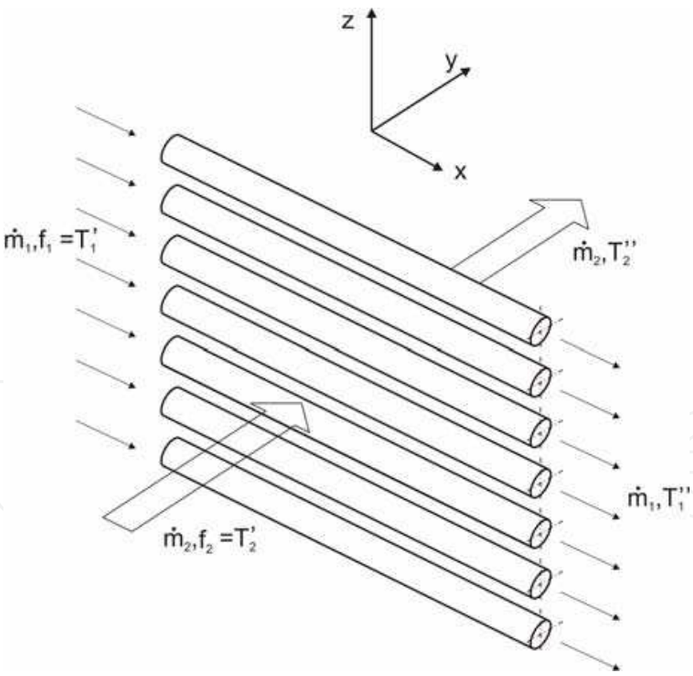

Fig. 1. One-row cross-flow tube heat exchanger

The numbers of heat transfer units N_1 and N_2 are given by

$$N_1=\frac{h_1A_{wrg}}{\dot{m}_1c_{p1}},\ N_2=\frac{h_oA_{zrg}}{\dot{m}_2c_{p2}},$$

The time constants τ_1, τ_w, τ_f, and τ_2 are

$$\tau_1 = \frac{m_1 c_{p1}}{h_1 A_{wrg}},\ \tau_w = \frac{\left(m_w + \eta_f m_f\right)c_w}{h_1 A_{wrg} + h_o A_{zrg}},\ \tau_f = \frac{\left(1-\eta_f\right)m_f c_w}{h_1 A_{wrg} + h_o A_{zrg}},\ \tau_2 = \frac{m_2 c_{p2}}{h_o A_{zrg}},$$

$$m_1 = n_{rg} A_w L_{ch} \rho_1,\ m_2 = n_{rg}\left(p_1 p_2 - A_{oval}\right)\left(s-\delta_f\right)n_f \rho_2,\ m_w = n_{rg} U_m \delta_w L_{ch} \rho_w$$

$$m_f = n_{rg} n_f \left(p_1 p_2 - A_{oval}\right)\delta_f \rho_w,\ A_w = \pi a b,\ A_{oval} = \pi\left(a+\delta_w\right)\left(b+\delta_w\right),\ U_m = \left(U_w + U_z\right)/2\ .$$

The weighted heat transfer coefficient h_o is defined by

$$h_o = h_2\left[\ \frac{A_{mf}}{A_{zrg}} + \frac{A_f}{A_{zrg}}\eta_f(\ h_2\ )\ \right]\quad . \tag{5}$$

The symbols in Equations (1-5) denote: a, b - minimum and maximum radius of the oval inner surface; A_f - fin surface area; A_{mf} - area of the tube outer surface between fins; A_{oval}, A_w - outside and inside cross section area of the oval tube; $A_{wrg} = n_{rg} U_w L_{ch}$, $A_{zrg} = n_{rg} U_z L_{ch}$ - inside and outside surface area of the bare tube; c_p - specific heat at constant pressure; c_w - specific heat of the tube and fin material; h_1 and h_2 - water and air side heat transfer coefficients, respectively; h_o - weighted heat transfer coefficient from the air side related to outer surface area of the bare tube; L_{ch} - tube length in the automotive radiator; m_1, m_2, m_f and m_w - mass of the water, air, fins, and tube walls in the heat exchanger, $\dot{m}_1$ - mass flow rate of cooling liquid flowing inside the tubes; $\dot{m}_2$ - air mass flow rate; n_f - number of fins on the tube length; n_{rg} - number of tubes in the heat exchanger; N_1 and N_2 – number of heat transfer units for water and air, respectively; p_1 - pitch of tubes in plane perpendicular to flow (height of fin); p_2 - pitch of tubes in direction of flow (width of fin); s - fin pitch; t - time; T_1, T_w and T_2 - water, tube wall and air temperature, respectively; U_w and U_z - inner and outer tube perimeter of the bare tube, η_f - fin efficiency, $x^+ = x/L_{ch}$, $y^+ = y/p_2$ - dimensionless Cartesian coordinates; δ_f and δ_w - fin and tube thickness, respectively; ρ - density; τ_1, τ_w, τ_f and τ_2 - time constants.
The initial temperature distributions of the both fluids $T_{1,0}\left(x^+\right)$, $T_{2,0}\left(x^+, y^+\right)$ and the wall $T_{w,0}\left(x^+\right)$ are known from measurements or from the steady-state calculations of the heat exchanger. The initial conditions are defined as follows

$$T_1\left(x^+, t\right)\big|_{t=0} = T_{1,0}\left(x^+\right), \tag{6}$$

$$T_w\left(x^+, t\right)\big|_{t=0} = T_{w,0}\left(x^+\right), \tag{7}$$

$$T_2\left(x^+, y^+, t\right)\big|_{t=0} = T_{2,0}\left(x^+, y^+\right). \tag{8}$$

The boundary conditions have the following form

$$T_1\left(x^+,t\right)\Big|_{x^+=0} = f_1\left(t\right), \tag{9}$$

$$T_2\left(x^+,y^+,t\right)\Big|_{y^+=0} = f_2\left(t\right), \tag{10}$$

where $f_1(t)$ and $f_2(t)$ are functions describing the variation of the temperatures of inlet liquid and air in time. The initial-boundary value problem formulated above (1–10) applies to heat exchangers made of smooth tubes and also from finned ones. The transient fluids and wall temperature distributions in the one row heat exchanger (Fig. 1) are then determined by the explicit finite difference method and by Laplace transform method.

2.1.1 Explicit finite difference method

When actual heat exchangers are calculated, the thermo-physical properties of the fluids and the heat transfer coefficients depend on the fluid temperature, and the initial boundary problem (1–10) is non-linear. In such cases, the Laplace transform cannot be applied. The temperature distribution $T_1\left(x^+,t\right)$, $T_w\left(x^+,t\right)$, and $T_2\left(x^+,y^+,t\right)$ can then be found by the explicit finite difference method. The time derivative is approximated by a forward difference, while the spatial derivatives are approximated by backward differences. The equations (1–3) are approximated using the explicit finite difference method

$$\frac{1}{N_1^n}\frac{T_{1,i+1}^n - T_{1,i}^n}{\Delta x^+} + \tau_1^n \frac{T_{1,i+1}^{n+1} - T_{1,i+1}^n}{\Delta t} = -\left(\frac{T_{1,i}^n + T_{1,i+1}^n}{2} - T_{w,i}^n\right), \tag{11}$$

$i = 1, \ldots, N$, $n = 0, 1, \ldots$

$$\tau_w^n \frac{T_{w,i}^{n+1} - T_{w,i}^n}{\Delta t} + \tau_f^n \frac{T_{m2,i}^{n+1} - T_{m2,i}^n}{\Delta t} + T_{w,i}^n = \frac{h_1^n U_w}{h_1^n U_w + h_o^n U_z}\frac{T_{1,i}^n + T_{1,i+1}^n}{2} + \frac{h_o^n U_z}{h_1^n U_w + h_o^n U_z} T_{m2,i}^n, \tag{12}$$

$i = 1, \ldots, N$, $n = 0, 1, \ldots$

$$\frac{1}{N_2^n}\frac{\left(T'_{2,i}\right)^n - \left(T''_{2,i}\right)^n}{1} + \tau_2^n \frac{\left(T''_{2,i}\right)^{n+1} - \left(T''_{2,i}\right)^n}{\Delta t} = T_{w,i}^n - \frac{\left(T'_{2,i}\right)^n + \left(T''_{2,i}\right)^n}{2}, \tag{13}$$

$i = 1, \ldots, N$, $n = 0, 1, \ldots$.

The nodes are shown in Fig. 2. The designations are as follows

$$W1(I) = T_{1,i},\ P1(I) = T'_{2,i},\ P2(I) = T''_{2,i},\ R1(I) = T_{w,i}.$$

The unknown temperature $T_{1,i+1}^{n+1}$ is found from Eq. (11), $T_{w,i}^{n+1}$ from Eq. (12), and $\left(T''_{2,i}\right)^{n+1}$ from Eq. (13):

$$T_{1,i+1}^{n+1} = T_{1,i+1}^n - \frac{\Delta t}{N_1^n \tau_1^n}\frac{T_{1,i+1}^n - T_{1,i}^n}{\Delta x^+} - \frac{\Delta t}{\tau_1^n}\left(\frac{T_{1,i}^n + T_{1,i+1}^n}{2} - T_{w,i}^n\right), \tag{14}$$

$i = 1, \ldots, N$, $n = 0, 1, \ldots$

$$T_{w,i}^{n+1} = T_{w,i}^{n} + \frac{\Delta t}{\tau_w^n}\left\{ \frac{h_1^n A_{wrg}}{h_1^n A_{wrg} + h_o^n A_{zrg}} \frac{T_{1,i}^n + T_{1,i+1}^n}{2} + \frac{h_o^n A_{zrg}}{h_1^n A_{wrg} + h_o^n A_{zrg}} \frac{\left(T'_{2,i}\right)^n + \left(T''_{2,i}\right)^n}{2} - T_{w,i}^n - \right.$$

$$\left. - \frac{\tau_f^n}{\Delta t}\left[\frac{\left(T'_{2,i}\right)^{n+1} + \left(T''_{2,i}\right)^{n+1}}{2} - \frac{\left(T'_{2,i}\right)^n + \left(T''_{2,i}\right)^n}{2} \right] \right\}, \tag{15}$$

$i = 1, \ldots, N$, $n = 0, 1, \ldots$

$$\left(T''_{2,i}\right)^{n+1} = \left(T''_{2,i}\right)^n + \frac{\Delta t}{N_2^n \tau_2^n}\left[\left(T'_{2,i}\right)^n - \left(T''_{2,i}\right)^n\right] + \frac{\Delta t}{\tau_2^n}\left[T_{w,i}^n - \frac{\left(T'_{2,i}\right)^n + \left(T''_{2,i}\right)^n}{2} \right], \tag{16}$$

$i = 1, \ldots, N$, $n = 0, 1, \ldots$

where Δt is the time step and the dimensionless spatial step is: $\Delta x^+ = 1/N$.

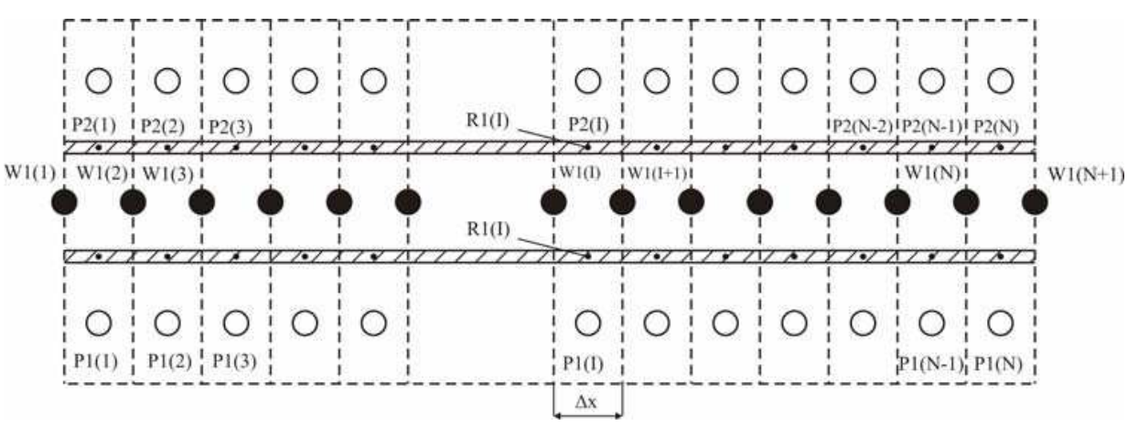

Fig. 2. Diagram of nodes in the calculation of temperature distribution by the finite difference method; P1(I)–inlet air temperature, R1(I)–tube wall temperature, P2(I)–outlet air temperature

The initial conditions (6–8) and the boundary conditions (9, 10) assume the form:

- initial conditions

$$T_{1,i}^0 = T_{1,0}\left(x_i^+\right), \; n = 0, \; i = 1, \ldots, N+1, \tag{17}$$

$$T_{w,i}^0 = T_{w,0}\left(x_i^+\right), \; i = 1, \ldots, N \tag{18}$$

$$\left(T'_{2,i}\right)^0 = T'_{2,0}\left(x_i^+\right), \; i = 1, \ldots, N, \tag{19}$$

$$\left(T''_{2,i}\right)^0 = T''_{2,0}\left(x_i^+\right), \; i = 1, \ldots, N, \tag{20}$$

where $x_i^+ = (i-1)\Delta x^+$, $i = 1, \ldots, N+1$.

- boundary conditions

$$T_{1,1}^n = f_1^n,\ n = 0,1,..., \tag{21}$$

$$\left(T'_{2,i} \right)^n = f_2^n,\ n = 0,1,..., \tag{22}$$

where $f_1^n = f_1\left(n\Delta t \right)$, $f_2^n = f_2\left(n\Delta t \right)$.
In order to ensure stability of the calculations by the explicit finite difference method, the conditions of Courant (Press et al. , 2006; Taler, 2009) must be satisfied

$$\frac{\Delta t}{N_1^n \tau_1^n \Delta x^+} \le 1, \tag{23}$$

$$\frac{\Delta t}{N_2^n \tau_2^n} \le 1. \tag{24}$$

Because of the high air flow velocity w_2, the time step Δt resulting from the condition (24) should be very small, in the range of tens of thousandths of a second. The temperature distribution is calculated using the formulas (14–16) taking into consideration the initial (17–20) and boundary conditions (21–22), and starting at n = 0.

2.1.2 Laplace transform method

Applying the Laplace transform for the time t in the initial boundary problem (1–10) leads to the following boundary problem

$$\frac{1}{N_1}\frac{d\overline{T}_1}{d x^+} + \tau_1\left(s\overline{T}_1 - T_{1,0} \right) = -\left(\overline{T}_1 - \overline{T}_w \right), \tag{25}$$

$$\tau_w\left(s\overline{T}_w - T_{w,0} \right) + \tau_f\left(s\overline{T}_{m2} - T_{m2,0} \right) + \overline{T}_w = \frac{h_1 U_w}{h_1 U_w + h_o U_z}\overline{T}_1 + \frac{h_o U_z}{h_1 U_w + h_o U_z}\overline{T}_{m2}, \tag{26}$$

$$\frac{1}{N_2}\frac{\partial \overline{T}_2}{\partial y^+} + \tau_2\left(s\overline{T}_2 - T_{2,0} \right) = \overline{T}_w - \overline{T}_2, \tag{27}$$

$$\overline{T}_1\left(x^+, s \right)\Big|_{x^+=0} = \overline{f}_1\left(s \right), \tag{28}$$

$$\overline{T}_2\left(x^+, y^+, s \right)\Big|_{y^+=0} = \overline{f}_2\left(s \right), \tag{29}$$

where the Laplace transform of the function $F(t)$ is defined as follows

$$\overline{F}\left(s \right) = \int_0^\infty e^{-st} F\left(t \right) dt. \tag{30}$$

The symbol s in Equations (25-30) denotes the complex variable.

Solving the equations (25–27) with boundary conditions (28–29) and the initial condition

$$T_{1,0} = T_{w,0} = T_{2,0} = T_{m2,0} = 0 \tag{31}$$

gives

$$\overline{T}_1 = (R/\tau)\left(1 - e^{-\tau N_1 x^+}\right) + \overline{f}_1(s)\, e^{-\tau N_1 x^+}, \tag{32}$$

$$\overline{T}_w = \frac{E\overline{T}_1 + \left[G\overline{f}_2(s)/H\right]\left(1 - e^{-H}\right)}{1 - GN_2\left[1/H - \left(1/H^2\right)\left(1 - e^{-H}\right)\right]}, \tag{33}$$

$$\overline{T}_2 = \overline{f}_2(s)\, e^{-(1+s\tau_2)N_2 y^+} + \frac{\overline{T}_w}{1+s\tau_2}\left[1 - e^{-(1+s\tau_2)N_2 y^+}\right], \tag{34}$$

where

$$\tau = s\tau_1 + 1 - \frac{E}{1 - GN_2\left[1/H - \left(1/H^2\right)\left(1 - e^{-H}\right)\right]},$$

$$E = \frac{h_1 A_{wrg}}{h_1 A_{wrg} + h_o A_{zrg}} \cdot \frac{1}{\tau_w s + 1},$$

$$G = \left(\frac{h_0 A_{zrg}}{h_1 A_{wrg} + h_o A_{zrg}} - \tau_f s\right)\frac{1}{\tau_w s + 1},$$

$$H = (1 + s\tau_2)N_2,$$

$$R = \frac{\left[G\overline{f}_2(s)/H\right]\left(1 - e^{-H}\right)}{1 - GN_2\left[1/H - \left(1/H^2\right)\left(1 - e^{-H}\right)\right]}.$$

The transforms of the solutions $\overline{T}_1 = \overline{T}_1\left(x^+, s\right)$, $\overline{T}_w = \overline{T}_w(x^+, s)$ and $\overline{T}_2 = \overline{T}_2\left(x^+, y^+, s\right)$ are complex and therefore the inverse Laplace transforms of the functions $\overline{T}_1$ and $\overline{T}_2$ are determined numerically by the method of Crump (Crump, 1976) improved by De Hoog (De Hoog 1982). The transforms of the solutions $\overline{T}_1$, $\overline{T}_w$ and $\overline{T}_2$ are found under the assumption that the discussed problem is linear, i.e. that the coefficients N_1, τ_1, N_2, τ_2, τ_w and τ_f in the equations (1–3) are independent of temperature. In view of the high accuracy of the solution obtained by the Laplace transform, it can be applied to verify the approximate solutions obtained by the method of finite differences.

3. Test calculations

A step change of air inlet temperature in one tube row of the exchanger, from the initial temperature T_0 to $T_0 + \Delta T_2$ will be considered. The design of the exchanger is shown in the

paper (Taler 2002, Taler 2009). The discussed exchanger consists of ten oval tubes with external diameters $d_{\min} = 2 \cdot (a + \delta_w) = 6.35$ mm and $d_{\max} = 2 \cdot (b + \delta_w) = 11.82$ mm. The thickness of the aluminium wall is δ_w = 0.4 mm. The tubes are provided with smooth plate fins with a thickness of δ_f = 0.08 mm and width of p_2 = 17 mm. The height of the tube bank is $H = n_r p_1$ = 10 × 18.5 = 185 mm, where n_r = 10 denotes the number of tubes, and p_1 is the transverse tube spacing. Water flows inside the tubes and air on their outside, perpendicularly to their axis. The pipes are L_x = 0.52 m long. The initial temperature are: $T_{1,0} = T_{w,0} = T_{2,0}$ = 0°C. For time t > 0, the sudden temperature increase by ΔT_2 = 10°C occurs on the air-side before the heat exchanger. The water temperature f_1 at the inlet to the exchanger tubes is equal to the initial temperature T_0 = 0°C.

The flow rate of water is constant and amounts $\dot{V}_1$ = 1004 l/h. The air velocity in the duct before the exchanger is w_2 = 7.01 m/s and the velocity in the narrowest cross section between two tubes is $w_{\max}$ = 11.6 m/s. The mass of water in the tubes is m_1 = 0.245 kg and the mass of tubes including fins is (m_w + m_f) = 0.447 kg. The time constants are τ_1 = 5.68 s, τ_2 = 0.0078 s, τ_f = 0 s, τ_w = 1.0716 s and the numbers of heat transfer units N_1 and N_2 are equal to N_1 = 0.310, N_2 = 0.227. The heat transfer coefficients are: h_1 = 1297.1 W/(m²K), h_2 = 78.1 W/(m²K).

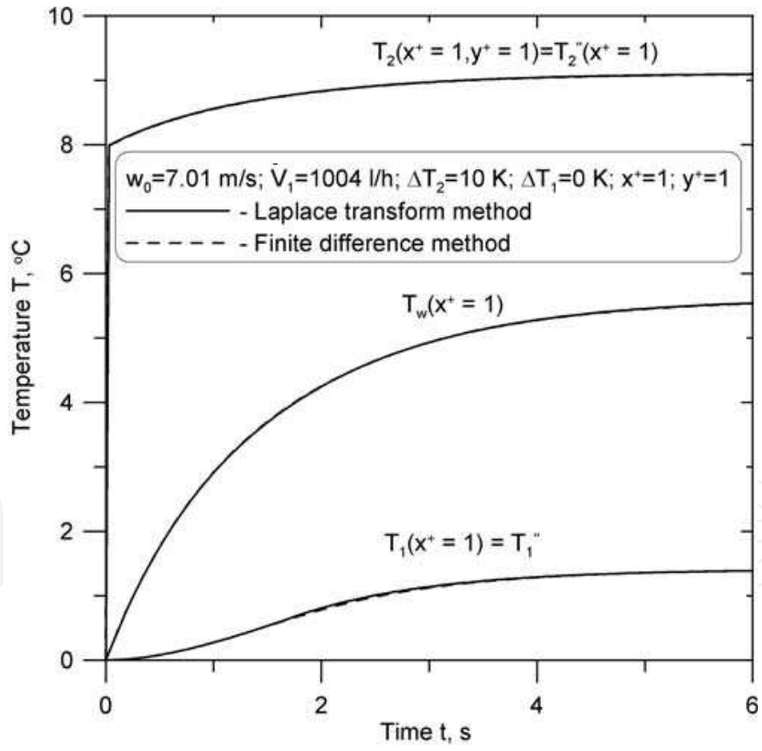

Fig. 3. Plot of temperatures of water $T_1(x^+ = 1)$, tube wall $T_w(x^+ = 1)$ and air $T_2(x^+ = 1, y^+ = 1)$ at the exchanger outlet ($x^+ = 1$, $y^+ = 1$)

The changes of the temperatures of water and air were determined by the method of Laplace transform and by the finite difference method. The water temperature on the tube length was determined in 21 nodes (N = 20, Δx^+ = 0.05). The time integration step was

assumed as Δt = 0.0001 s. The transients of water and air temperatures at the outlet of the exchanger (x^+ = 1, y^+ = 1) are presented in Fig. 3.

The water temperature distribution on the length of the exchanger at various time points is shown in Fig. 4. Comparing the plots of air, tube wall and water at the exchanger outlet indicates that the results obtained by the Laplace transform method and the finite difference method are very close. The air outlet temperature in the point x^+ = 1, y^+ = 1 is close to temperature in steady state already after the time t = 3.9 s. Figure 3 shows that the air temperature past the row of tubes (x^+ = 1, y^+ = 1) is already almost equal to the steady state temperature after a short time period when the inlet air arrives at the outlet of the heat exchanger. The steady-state water temperature increases almost linearly from the inlet of the heat exchanger to its outlet. It is evident that the accuracy of the results obtained by the finite difference method is quite acceptable.

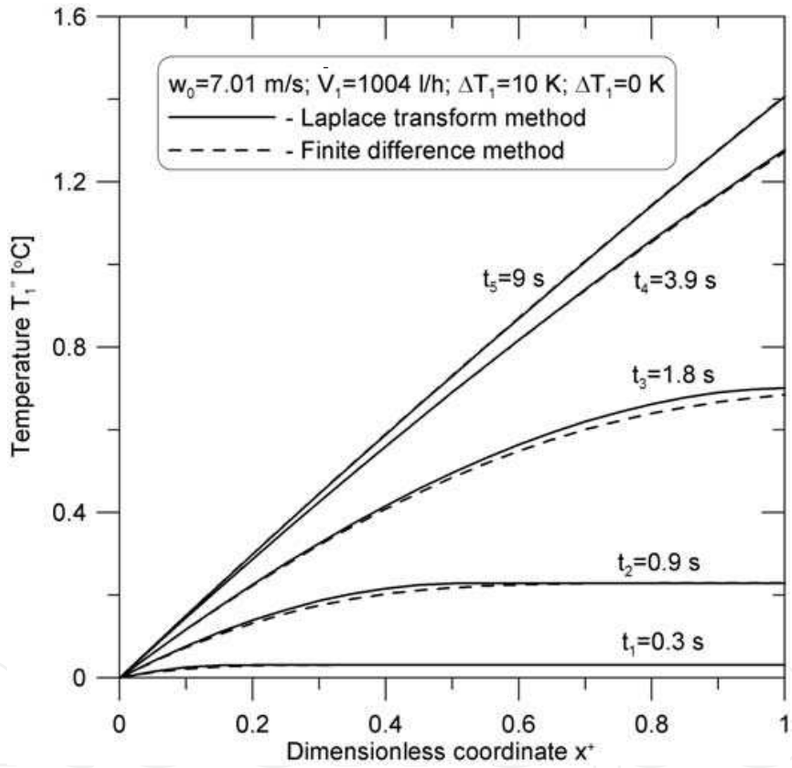

Fig. 4. Comparison of water temperatures on the tube length determined by the finite difference method and the Laplace transform method

4. The numerical model of the heat exchanger

The automotive radiator for the spark-ignition combustion engine with a cubic capacity of 1580 cm^3 is a double-row, two-pass plate-finned heat exchanger. The radiator consists of aluminium tubes of oval cross-section. The cooling liquid flows in parallel through both tube rows. Figures 5a-5c show a diagram of the two-pass cross-flow radiator with two rows of tubes. The heat exchanger consists of the aluminium tubes of oval cross-section.

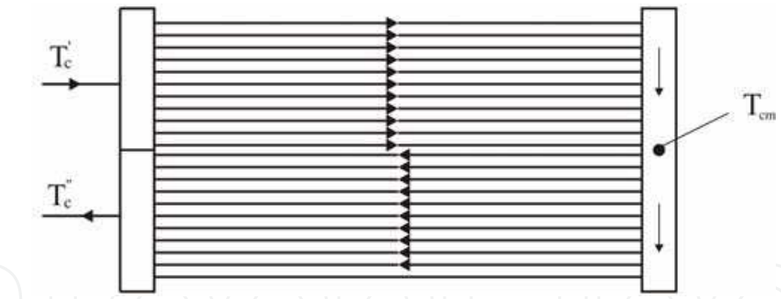

(a)

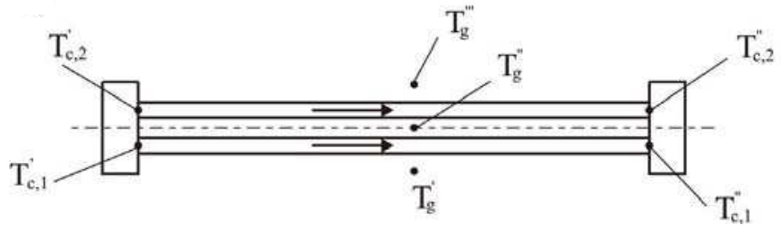

(b)

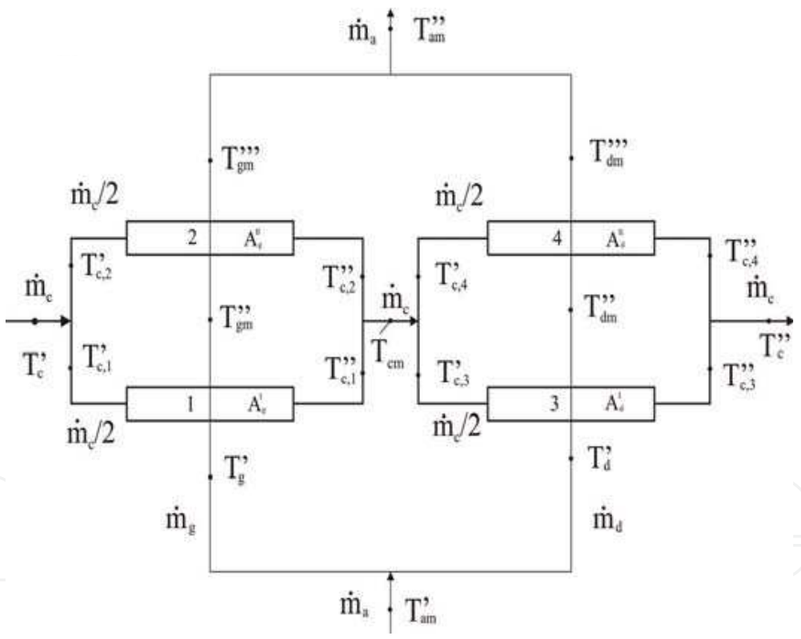

(c)

1 – first tube row in upper (first) pass, 2 – second tube row in upper pass; 3 – first tube row in lower (second) pass, 4 – second tube row in lower pass; T'_w and T''_w - inlet and outlet water temperature, respectively, T'_{am} and T''_{am} - inlet and outlet air mean temperature, respectively, $\dot{m}_a$, $\dot{m}_w$ - air and water mass flow rate at the inlet of the heat exchanger, respectively

Fig. 5. Two-pass plate-fin and tube heat exchanger with two in-line tube rows;

The outlets from the upper pass tubes converge into one manifold. Upon mixing the cooling liquid with the temperature $T'_1(t)$ from the first tube row and the cooling liquid with the

temperature T_2'' from the second tube row, the feeding liquid temperature of the second, lower pass is $T_{cm}(t)$. In the second, lower pass, the total mass flow rate splits into two equal flow rates $\dot{m}_c / 2$. On the outlet from the first tube row in the bottom pass the coolant temperature is $T_3''(t)$, and from the second row is $T_4''(t)$. Upon mixing the cooling liquid from the first and second row, the final temperature of the coolant exiting the radiator is $T_c''(t)$. The air stream with mass flow rate $\dot{m}_a(t)$ flows crosswise through both tube rows. Assuming that the air inlet velocity w_0 is in the upper and lower pass, the mass rate of air flow through the upper pass is $\dot{m}_g = \dot{m}_a n_g / n_t$, where n_g is the number of tubes in the first row of the upper pass and n_t is the total number of tubes in the first row of the upper and lower pass. The air mass flow rate across the tubes in the lower pass is $\dot{m}_d = \dot{m}_a n_d / n_t$, where n_d is the number of tubes in the first row of the lower pass. A discrete mathematical model, which defines the transient heat transfer was obtained using the control volume method. Figure 6a shows the division of the first pass (upper pass) into control volumes and Figure 6b the division of the second pass (lower pass).

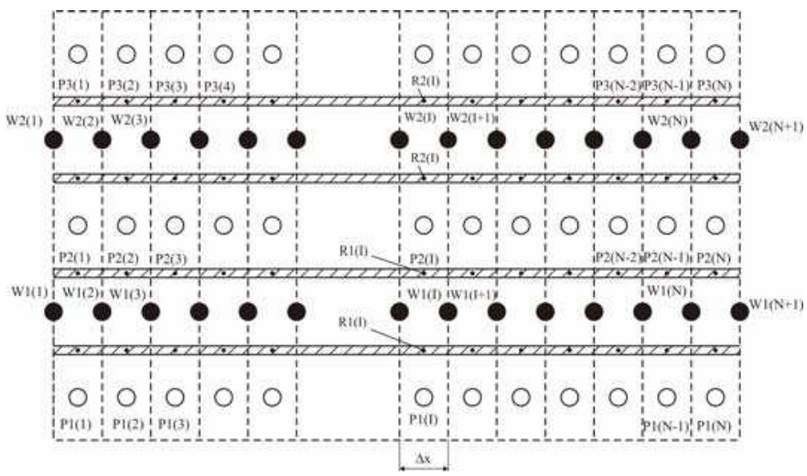

(a)

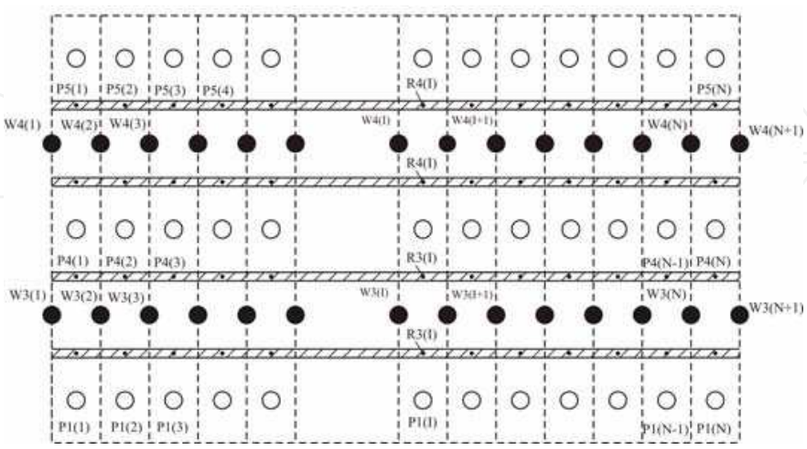

(b)

Fig. 6. Division of the first and second pass of the car radiator into control volumes; a) first pass, b) second pass, ◦ - air temperature, • - cooling liquid temperature

In order to increase the accuracy of the calculations, a staggered mesh will be applied. Liquid temperatures at the control volume nodes are denoted by W1(I) and W2(I) for the first and second rows of tubes, respectively. P1(I) denotes air temperature $T'_{g,i} = T'_{am}(t)$ in front of the radiator, P2(I) denotes air temperature $T''_{g,i}$ after the first row of tubes and P3(I) air temperature $T'''_{g,i}$ after the second row of tubes in the i -th control volume. The coolant temperature flowing through the first and second row, in the upper and lower pass, is a function of the coordinate *x* and time *t*, only. Temperatures $T'_{am}(t)$ and $T'''_{am}(t)$ denote the mean values of the radiator's inlet and outlet air temperatures, respectively. In order to determine transient temperature distribution of the water, tube wall and air, the finite difference method described in section 2.1 was used. For the analysis, the liquid temperature at the inlet to the first and second row of tubes in the upper pass was considered to be $T'_c(t)$ and $T_{cm}(t)$ in the lower pass. Using the notation shown in Figures 6a and 6b, the boundary conditions can be written in the following form

$$W1(1) = W2(1) = T'_1(t) = T'_2(t) = T'_c(t), \quad P1(I) = T'_{am}(t) = T'_{gm}(t) \quad I = 1,...,N . \tag{35}$$

The inlet air velocity w_0 and mass flow rate $\dot{m}_c$ are also functions of time. In the simulation program the time variations of: $T'_c(t)$, $T'_{am}(t)$, $w_0(t)$, and $\dot{m}_c(t)$ were interpolated using natural splines of the third degree.

The temperature $T_{cm}(t)$ is a temperature of the liquid at the outlet of the upper pass, where the liquid of temperature $W1(N+1)$ from the first row of tubes has been mixed with the liquid of temperature $W2(N+1)$ flowing out of the second row of tubes. In the case of the automotive radiator, temperature $T'_c(t)$ denotes the liquid temperature (of the engine coolant) at the inlet to the radiator whereas $T'_{am}(t)$ denotes air temperature in front of the radiator. Having determined the mean temperatures of the air T'''_{gm} and T'''_{dm} leaving the second row of tubes in the upper and lower pass, respectively, a mean temperature of the air behind the whole radiator $T'''_{am} = \left(n_g T'''_{gm} + n_d T'''_{dm} \right) / n_t$ was calculated. If the liquid and air temperatures are known, the heat transfer rate in the first and second rows of tubes in the upper and lower passes can be determined. The total heat transfer rate for the radiator was calculated using the formula $\dot{Q}_{chl} = \dot{m}_c \left[i_c(T'_c) - i_c(T''_c) \right] = \dot{m}_a \bar{c}_a \left(T'''_{am} - T'_{am} \right)$. The symbols i_c and $\bar{c}_a$ denote the water enthalpy and air mean specific capacity, respectively. The numerical model of the heat exchanger described briefly above is used to simulate its transient operation. Before starting transient simulation, the steady-state temperature distribution of water, tube wall and air was calculated using the steady-state mathematical model of the heat exchanger presented in (Taler, 2002; Taler, 2009).

5. Experimental verification

In order to validate the developed model of the heat exchanger, an experimental test stand was built. The measurements were carried out in an open aerodynamic tunnel.

The experimental setup was designed to obtain heat transfer and pressure drop data from commercially available automotive radiators. The test facility follows the general guidelines presented in ASHRAE Standards 33-798 (ASHRAE, 1978) and 84-1991 (ANSI/ASHRAE, 1982). Air is forced through the open-loop wind tunnel by a variable speed centrifugal fan. The air flow passed the whole front cross-section of the radiator. A straightener was used to provide better flow distribution. Air temperature measurements were made with multipoint (nickel-chromium)-(nickel-aluminium) thermocouple grids (K type sheath thermocouple

grids). The thermocouples were individually calibrated. The 95% uncertainty of the thermocouples estimated during the isothermal test was ±0.3 K. The air flow was determined at two cross sections from measurement of the velocity pressure obtained by Pitot traverses (Taler, 2006b). Additionally, the air flow was measured by the averaging Pitot tube device. The uncertainty in the measured air mass flow rate is ±1.0%. The static pressure drop across the radiator was measured with the four-tap piezometer rings using a precision differential pressure transducer with the 95% uncertainty of the order of ±1 Pa. The hot water is pumped from the thermostatically controlled tank through the radiator by the centrifugal pump with a frequency inverter. Water flow rates were measured with a turbine flowmeter that was calibrated using a weighting tank. The 95% uncertainty in the flow measurement was of ±0.004 L/s. Water solution temperatures at the inlet and outlet of the radiator were measured with calibrated platinum resistance thermometers (Pt 100 sensors). The 95% uncertainty in the temperature measurement is about ±0.05 K. Liquid pressure at the inlet and outlet of the radiator was measured with temperature compensated piezo-resistive sensors with an uncertainty of ±0.5 kPa. A personal computer-based data-acquisition system was used to measure, store and interpret the data. The relative difference between the air-side and liquid-side heat transfer rate was less than 3%. Extensive heat transfer measurements under steady-state conditions were conducted to find the correlations for the air- and water-side Nusselt numbers, which enable the calculation of heat transfer coefficients. Based on 21 measurement series, the following correlations were identified

$$Nu_c = \frac{(\xi/8)(\mathrm{Re}_c - 33.6625)\mathrm{Pr}_c}{(1 + 34.9622\sqrt{(\xi/8)}(\mathrm{Pr}_c^{2/3} - 1)}\left[1 + \left(\frac{d_r}{L_{ch}}\right)^{2/3}\right], \tag{36}$$

$$Nu_a = 0.01285\,\mathrm{Re}_a^{1.0755}\,\mathrm{Pr}_a^{1/3}, \tag{37}$$

where the friction factor ξ is given by

$$\xi = \frac{1}{(1.82\log\mathrm{Re}_c - 1.64)^2} = \frac{1}{(0.79\ln\mathrm{Re}_c - 1.64)^2}.$$

The water-side Reynolds number $\mathrm{Re}_c = w_c d_r / \nu_c$ is based on the hydraulic diameter $d_r = 4A_w / P_w$, where A_w denotes inside cross section area of the oval tube. The hydraulic diameter for the investigated radiator is: $d_r = 7.06 \cdot 10^{-3}$ mm.

The physical properties of air and water were approximated using simple functions. The effect of temperature-dependent properties is accounted for by evaluating all the properties at the mean temperature of air and water, respectively. The method of prediction of heat transfer correlations for compact heat exchangers is described in details in (Taler, 2005). Measurement results are shown in Fig. 7. Then, the transient response of the heat exchanger was analyzed. Using the measured values of: inlet water temperature T_c', inlet air temperature T_{am}', air velocity in front of the radiator w_0, and water volumetric flow rate $\dot{V}_c$, the water, tube wall and air temperatures are determined using the explicit finite difference method, presented in the section 2.1. The calculation results and their comparison with experimental data are shown in Fig. 8. The agreement between the calculated and measured water temperature at the outlet of the heat exchanger is very good. In the case of

the outlet air temperature larger differences between calculated and measured values are observed (Fig. 8).

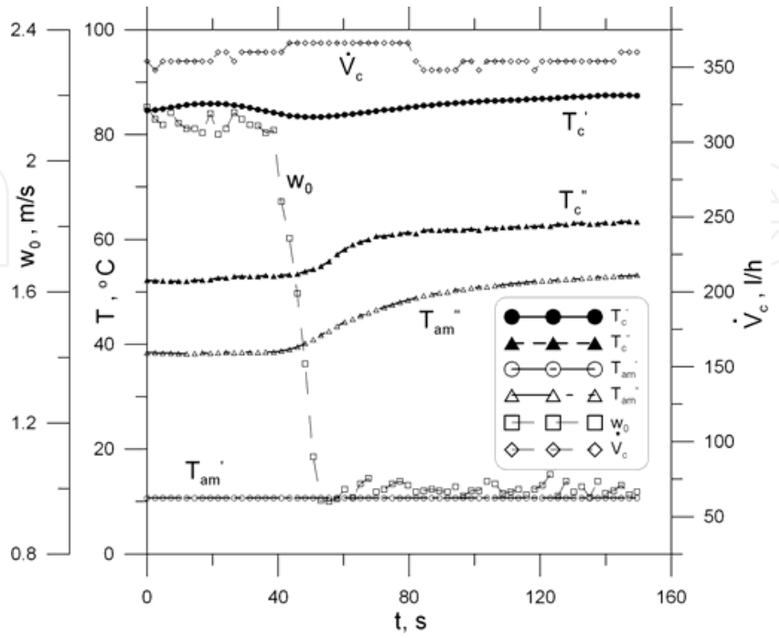

(a)

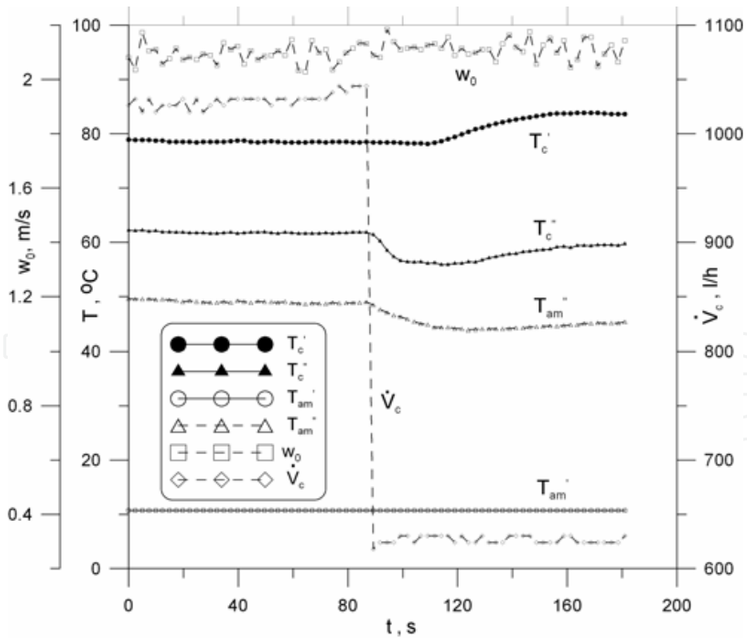

(b)

Fig. 7. Time variations of measured data: inlet water T_c' and air temperature T_{am}', respectively; outlet water T_c'' and air temperature T_{am}'', respectively; $\dot{V}_c$ - water mass flow rate, w_0 - air velocity before the heat exchanger

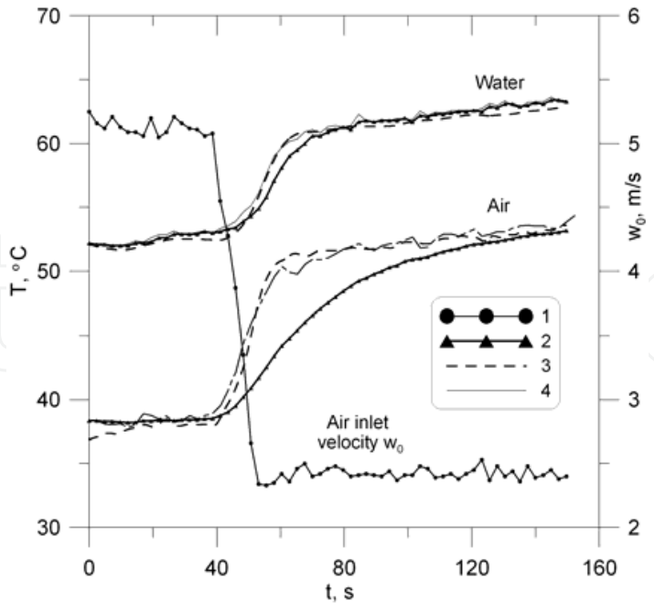

(a)

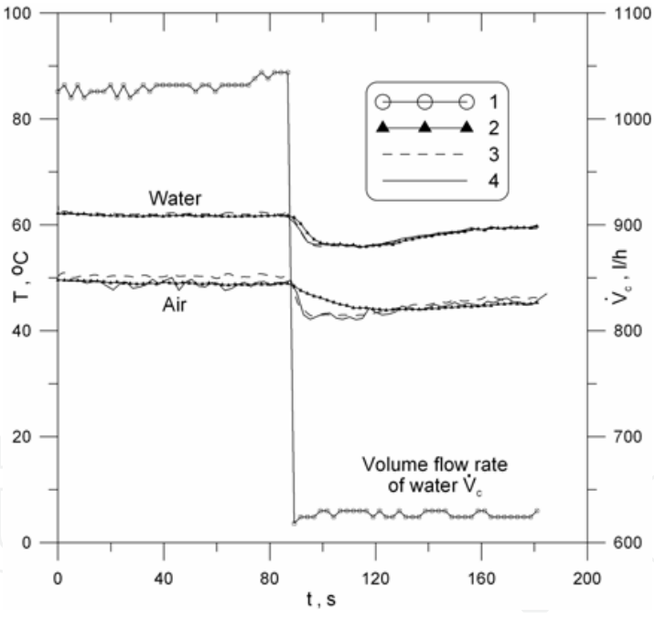

(b)

Fig. 8. Time variations of computed outlet water and air temperatures 1 - air velocity w_0 before the heat exchanger in Fig. a) and water volume flow rate $\dot{V}_c$ in Fig. b), 2 – outlet air and water temperatures indicated by thermocouples, 3 – computed air and water outlet temperatures, 4 – water and air outlet temperature calculated on the basis of measured value using the first order thermocouple model

This discrepancy is the result of damping and delay of air temperature changes by the sheath thermocouples of 1.5 mm diameter, used for the air temperature measurement. The

transient response of the thermocouple can be described by a simple first order differential equation

$$\tau_{th}\frac{dT_{th}}{dt}=T_f-T_{th}\,. \tag{38}$$

The symbols in equation (38) denote: T_f and T_{th} - fluid and thermocouple temperature, respectively, t - time, $\tau_{th}=m_{th}\,c_{th}\,/\left(h_{th}\,A_{th}\right)$ - time constant of the thermocouple, m_{th} - thermocouple mass, c_{th} - specific heat capacity of the thermocouple, h_{th} - heat transfer coefficient on the thermocouple surface, A_{th} - area of the outside surface of the thermocouple. Approximating time derivative in Eq. (38) by the central difference quotient and transforming Eq. (38) gives

$$T_f^n=T_{th}^n+\tau_{th}^n\frac{T_{th}^{n+1}-T_{th}^{n-1}}{2\Delta t_{th}}\,, \tag{39}$$

where the symbols in Eq. (39) stand for: $T_f^n=T_f\left(t\right)$, $T_{th}^n=T_{th}\left(t\right)$, $T_{th}^{n+1}=T_{th}\left(t+\Delta t_{th}\right)$, $T_{th}^{n-1}=T_{th}\left(t-\Delta t_{th}\right)$, Δt_{th} is the sampling time interval during temperature measurement by means of the data acquisition system. Taking into consideration that: τ_{th} = 20 s, Δt_{th} = 2.4 s, the air temperature is calculated using Eq. (39). An inspection of the results shown in Fig.8 indicates that the agreement between calculated and measured air temperature determined from Eq. (39) is very good. In the case of water temperature measurement, the time constant of the thermocouple is very small, since the heat transfer coefficient in the thermocouple surface is very high and the temperature indicated by the thermocouple and the real water temperature are very close.

6. Transient inverse heat transfer problem in control of plate fin and tube heat exchangers

In this section, a transient inverse heat transfer problem encountered in control of fluid temperature or heat transfer rate in a plate fin and tube heat exchanger was solved.

The water temperature $T_c''\left(t\right)$ at the outlet of the heat exchanger is known function of time. The problem to be solved is of great practical importance during start up and shut down processes of heat exchangers, internal combustion engines and in heating and ventilation systems. For example, the heat flow rate transferred from the internal combustion engine to cooling liquid is a function of time since it depends on the actual power of the engine, which in turn is a function of the car velocity and the slope of the road. Modern cooling systems are designed to maintain an even temperature at the outlet of the radiator despite of time dependent heat absorption by the engine coolant. This can be achieved by changing the fan rotating speed over time to keep the constant coolant temperature at the inlet of the engine. If the engine is operated at steady state conditions then its lifetime is much longer because thermal deformations and stresses are smaller.

The goal of the process control is to adjust the speed of fan rotation $n(t)$ in order that the water temperature $\left[T_c''(t)\right]^{cal}$ at the heat exchanger outlet is equal to a time-dependant target value (setpoint) $\left[T_c''(t)\right]^{set}$. The speed of rotation n is a function of time t and will be determined sequentially with a time step $\Delta t_B = t_M - t_{M-1}$. The method developed in the

paper can be easily extended to the control of heat flow rate transferred in the heat exchanger

$$\dot{Q}_c(t) = \dot{V}_c(t)\rho_c\left[T_c'(t)\right]\overline{c}_c\left[T_c'(t) - T_c''(t)\right], \tag{40}$$

where the symbols denote: $\dot{V}_c(t)$ - water volumetric flow rate at the heat exchanger inlet, ρ_c - water density, $\overline{c}_c$ - mean specific heat in the temperature range from $T_c''(t)$ to $T_c'(t)$. Solving equation (1) for $T_c''(t)$ gives

$$T_c''(t) = T_c'(t) - \frac{\dot{Q}_c(t)}{\dot{V}_c(t)\rho_c\left[T_c'(t)\right]\overline{c}_c}. \tag{41}$$

If the time changes of the heat flow rate $\dot{Q}_c(t)$ are prescribed as a function of time, then the inverse problem formulated with respect to the heat flow rate $\dot{Q}_c(t)$ is equivalent to the inverse problem formulated in terms of the water outlet temperature $T_c''(t)$.

6.1 Formulation of the inverse problem

The least squares method in conjunction with the first order regularization method are used for sequential determining the number of revolutions per minute

$$S(n_M) = \int_{t_{M-1}}^{t_{M+F}} \left[\left(T_{th,c}''\right)^{cal} - \left(T_{th,c}''\right)^{set} \right]^2 dt + w_r \left(\frac{dn}{dt}\Big|_{t=t_M} \right)^2 = \min, \tag{45}$$

where t is time, $\left(T_{th,c}''\right)^{cal}$ and $\left(T_{th,c}''\right)^{set}$ are the calculated and preset thermocouple temperature measuring water temperature at the outlet of the heat exchanger, w_r is the regularization parameter, and n denotes the speed of fan rotation. The sum (45) is minimized with respect to the number of fan revolutions per minute n_M at time t_M. Approximating the derivative in Eq. (45) by the forward difference quotient and the integral by the rectangle method gives

$$S(n_M) = \sum_{i=1}^{k_B(F+1)} \left\{ \left[T_{th,c}''(t_i)\right]^{cal} - \left[T_{th,c}''(t_i)\right]^{set} \right\}^2 + w_r \left(\frac{n_{M+F} - n_{M-1}}{t_{M+F} - t_{M-1}} \right)^2 = \min, \tag{46}$$

where (Fig. 1)

$$t_i = t_{M-1} + i\,\Delta t \quad , i = 1,\ldots, k_B\,(F+1). \tag{47}$$

The symbol F denotes the number of future time intervals (Fig. 1). Future time steps are used to stabilize the inverse problem for small time steps. Since the outlet temperature changes $\left(T_{th,c}''\right)^{cal}$ are delayed with reference to the changes of the speed of fan rotation n, the time interval $t_M - t_{M-1}$ was artificially extended to the value: $t_{M+F} - t_{M-1}$.

The future time steps were introduced to the inverse analysis by Beck (Beck, 2003) in order to make it possible to determine the unknown parameters with higher frequency. At first, the searched number of fan revolutions n_M is assumed to be constant over the whole time

interval $t_{M+F} - t_{M-1}$. After determining n_M from Eq. (46), the time interval $t_{M+F} - t_M$ is rejected and the estimated parameter n_M is taken only for the basic time interval $t_M - t_{M-1}$. The estimation of n_{M+1} starts from the time point t_M .

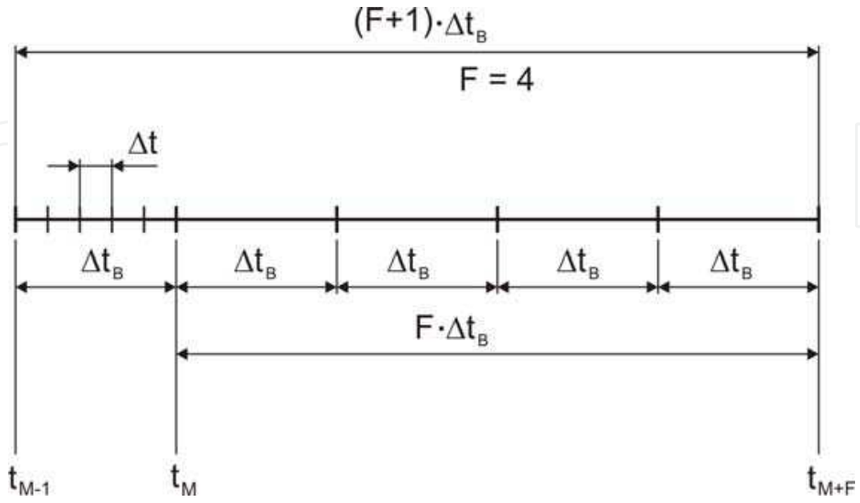

Fig. 9. Determination of speed of fan rotation n in the time interval $t_{M-1} \le t \le t_M$ using F future time intervals; Δt – time step in the finite difference method used in the mathematical model of the heat exchanger, $\Delta t_B = k_B \Delta t$ – basic time interval in the inverse analysis, F – number of future time intervals

The transient temperature of the thermocouple measuring the water temperature at the outlet of the heat exchanger $\left[T''_{th,c}(t_i)\right]^{cal}$ is calculated at every iteration step. The calculated thermocouple temperature $\left[T''_{th,c}(t_i)\right]^{cal}$ was determined from Eq. (38) using the explicit Euler method

$$\left[T''_{th,c}(t_i)\right]^{cal} = \left[T''_{th,c}(t_i - \Delta t_{th})\right]^{cal} + \left\{\left[T''_c(t_i - \Delta t_{th})\right]^{cal} - \left[T''_{th,c}(t_i - \Delta t_{th})\right]^{cal}\right\} \frac{\Delta t_{th}}{\tau_{th,c}}, \quad n = 0,1,... \quad (48)$$

A finite difference model of the investigated cross-flow tube heat exchanger, which enables heat transfer simulation under transient condition has been developed in section 4. This model was used for calculating $\left[T''_c(t_i - \Delta t_{th})\right]^{cal}$. If the thermocouple time constant $\tau_{th,c}$ is small, then from Eq. (38) results that the thermocouple temperature $\left[T''_{th,c}(t_i)\right]^{cal}$ is equal the water temperature $\left[T''_c(t_i)\right]^{cal}$.

The initial temperature distributions of the both fluids $T_{c,0}(x^+)$, $T_{a,0}(x^+, y^+)$ and the wall $T_{w,0}(x^+)$ are known from measurements or from the steady-state calculations of the heat exchanger. The boundary conditions have the following form (Fig. 2)

$$T_c(x^+, t)\big|_{x^+=0} = T'_c(t), \quad (49)$$

$$T_a(x^+, y^+, t)\big|_{y^+=0} = T'_{am}(t), \quad (50)$$

where $T_c'(t)$ and $T_{am}'(t)$ are functions describing the variation of the inlet temperatures of the water and air in time. In section 4, similar equations with appropriate boundary and initial conditions were formulated for four rows of the two row heat exchanger with two passes and solved using an explicit finite difference method. The numerical model was validated by comparison of outlet water and air temperatures obtained from the numerical simulation with the experimental data. The discrepancy between numerical and experimental results was very small.

6.2 Results

In order to demonstrate the effectiveness of the method presented in the subsection 6.1, the water temperature $\left(T_c''\right)^{set}$ at the outlet of the automotive radiator for the spark-ignition combustion engine with a cubic capacity of 1580 cm^3 was prescribed

$$\left(T_c''\right)^{set} = 52.0 + \frac{77.0 - 52.0}{118.22}\, t\,,\ 0 \le t \le 118.22\,, \tag{51}$$

$$\left(T_c''\right)^{set} = 77.0 - \frac{77.0 - 64.0}{31.36}\left(t - 118.22\right),\ 118.22 \le t \le 150.0\,, \tag{52}$$

where $\left(T_c''\right)^{set}$ is in °C and t is time in s.

The radiator consists of aluminium tubes of oval cross-section. The cooling liquid flows in parallel through both tube rows. Fig. 5 shows a diagram of the two-pass cross-flow radiator with two rows of tubes. The time changes of the water volumetric flow rate $\dot{V}_c$, air and water inlet temperatures T_{am}' and T_c' are shown in Fig. 7a.

The speed of fun rotation n and water outlet temperature $\left[T_c''(t)\right]^{cal}$ obtained from the solution of the inverse problem are also shown in Fig. 10. The air velocity w_0 was calculated using the simple experimental correlation

$$w_o = 0.001566 \cdot n - 0.0551, \quad 250 \le n \le 1440 \tag{53}$$

where w_0 is expressed in m/s and n in number of revolutions per minute (rpm).

The proposed method works very well, since the calculated water outlet temperature $\left[T_c''(t)\right]^{cal}$ and the preset temperature $\left[T_c''(t)\right]^{set}$ coincide (Fig. 10).

In order to validate the developed inverse procedure, an experimental test stand was built. The measurements were carried out in an open aerodynamic tunnel which is presented in section 5. The experimental setup was designed to obtain heat transfer and pressure drop data from commercially available automotive radiators.

The experimental results for sudden decrease in air velocity w_0 are shown in Fig. 7a. The water and air inlet temperatures $T_c'(t)$ and $T_{am}'(t)$, water volumetric flow rate $\dot{V}_c(t)$, and temperature of the thermometer measuring the water temperature at the outlet of the heat exchanger $\left[T_{th,c}''(t)\right]^{set} = T_{th,c}''(t)$ were used as the input data for the inverse analysis. The sampling time interval was Δt = 2.4 s. The data acquisition readings were interpolated using cubic splines. The solutions of the inverse problem and their comparison with experimental data are shown in Fig. 11.

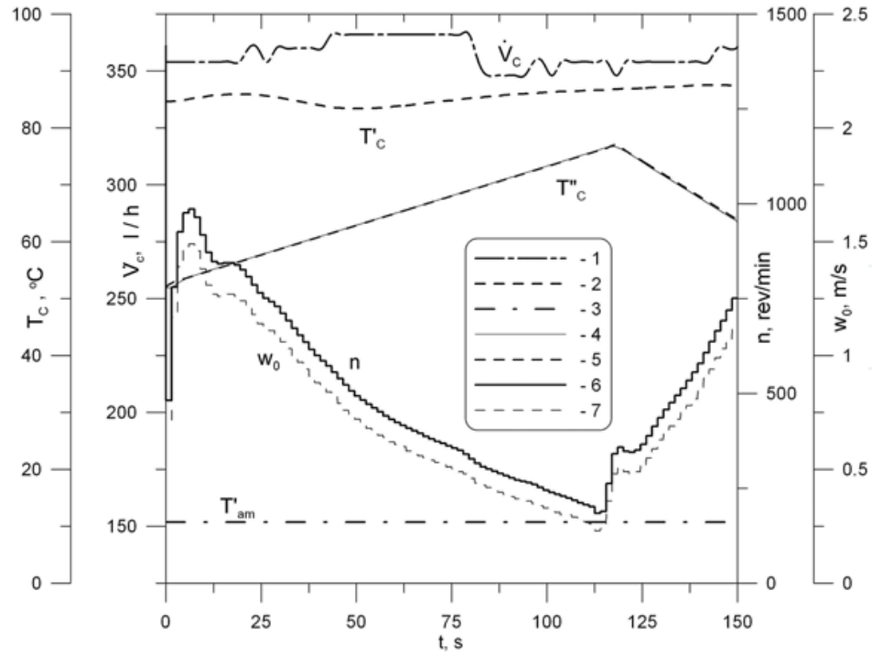

Fig. 10. Speed of fan rotation n (number of revolutions per minute), for which the calculated temperature $\left[T_c''(t)\right]^{cal}$ at the outlet of the heat exchanger is equal to preset temperature ; Δt = 0.05 s, k_B = 30, F = 2, w_r = 0; 1 – $\dot{V}_c$ - water mass flow rate at the inlet of the heat exchanger, 2 – T_c'' - water temperature at the inlet of the heat exchanger, 3 – T_{am}' - air temperature before the heat exchanger, 4 – calculated water temperature $\left[T_c''(t)\right]^{cal}$ obtained from the inverse solution, 5 – preset water temperature $\left[T_c''(t)\right]^{set}$ at the outlet of the heat exchanger, 6 – speed of fan rotation n determined from the inverse solution, 7 – air velocity before the heat exchanger based on the inverse solution for n

Despite different basic time intervals Δt_B and different number of future time intervals F very similar results are obtained (Fig. 11a and 11b). The agreement between the calculated and measured water temperature at the outlet of the heat exchanger is excellent.

7. Conclusions

The numerical models of cross-flow tube heat exchangers, which enable heat transfer simulation under transient condition were developed. First, the transient temperature distributions of fluids and tube wall in the one row tubular cross flow heat exchanger was determined using the finite difference method and the Laplace transform method. The results achieved by both methods were in good agreement. Then, the numerical model of the two row heat exchanger with two passes was presented. The numerical model was validated by comparison of outlet water and air temperatures obtained from the numerical simulation with the experimental data. The discrepancy between numerical and experimental results is very small.

In addition, a transient inverse heat transfer problem encountered in control of fluid temperature or heat transfer rate in a plate fin and tube heat exchanger was solved. The objective of the process control is to adjust the speed of fan rotation, measured in number of

fan revolutions per minute, so that the water temperature at the heat exchanger outlet is equal to a time-dependant target value (setpoint). The least squares method in conjunction with the first order regularization method was used for sequential determining the number of revolutions per minute. Future time steps are used to stabilize the inverse problem for small time steps. The transient temperature of the water at the outlet of the heat exchanger was calculated at every iteration step using a numerical mathematical model of the heat exchanger. The obtained solution, that is the speed of fan rotation, is very stable because of using future time steps and the first order regularization.

The method for solving the inverse problem developed in the paper was validated by comparing the calculated and measured number of fan revolutions per minute. The discrepancies between the calculated and measured revolution numbers are small.

The inverse method presented in the paper can be used for the solution of the inverse problems encountered in control of heat exchangers.

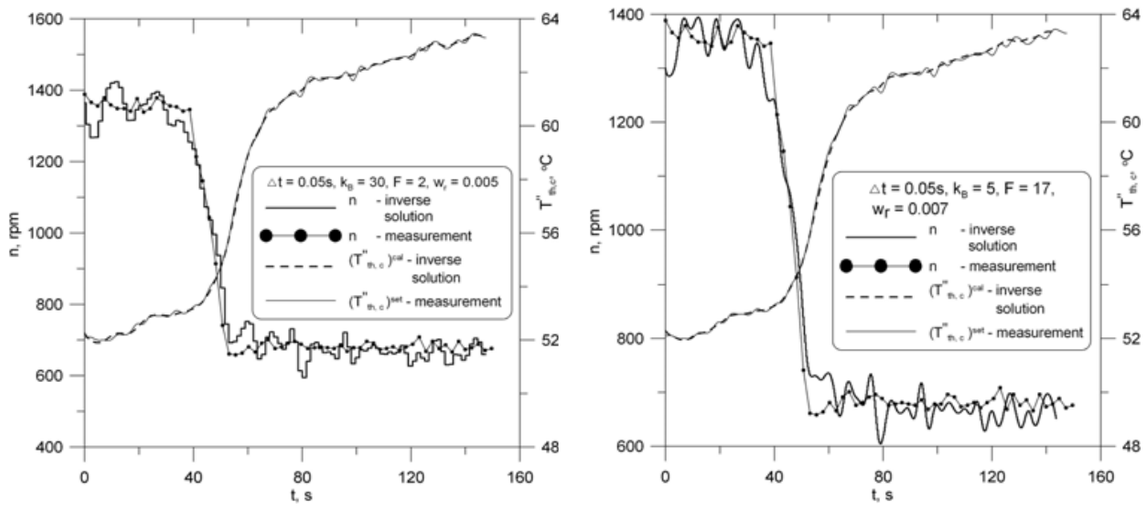

(a) (b)

Fig. 11. Speed of fan rotation n (number of revolutions per minute), for which the calculated temperature $\left[T''_{th,c}(t_i)\right]^{cal}$ at the outlet of the heat exchanger is equal to measured temperature $\left[T''_{th,c}(t_i)\right]^{set}$; a) Δt = 0.05 s, k_B = 30, F = 2, w_r = 0.005 $K^2s^2\,\mathrm{min}^2/rev^2$, b) Δt = 0.05 s , k_B = 5, F = 17, w_r = 0.007 $K^2s^2\,\mathrm{min}^2/rev^2$

8. References

ANSI/ASHRAE 84-1991. (1992). *Method of Testing Air-to-Air Heat Exchangers*. American Society of Heating, Refrigerating and Air-Conditioning Engineers, Inc., 1791 Tullie Circle, NE, Atlanta GA 30329, USA

ASHRAE Standard 33-798. (1978). *Methods of testing forced circulation air cooling and air heating coils.* American Society of Heating, Refrigerating and Air-Conditioning Engineers, Inc., Atlanta, USA

Beck, J. (2003). Sequential methods in parameter estimation, In: *Inverse Engineering Handbook*, Woodbury, K. A., (Ed.), 1-40, ISBN:0-8493-0861-5, CRC Press, Boca Raton, USA

Crump, K. S. (1976). Numerical inversion of Laplace transforms using a Fourier series approximation. *Journal of the Association of Computing Machinery*, Vol. 23, No. 1, 89-96, ISSN: 0004-5411

De Hoog, F. R.; Knight, J. H. & Stokes, A. N. (1982). An improved method for the numerical inversion of Laplace transforms. *SIAM Journal on Scientific and Statistical Computing*, Vol. 3, 357-366, ISSN: 0196-5204

Hesselgreaves, J. E. (2001) *Compact Heat Exchangers, Selection, Design and Operation*, Elsevier-Pergamon , ISBN: 0-08-042839-8, Oxford

Kraus A. D., Aziz A. & Welty J. (2001). *Extended Surface Heat Transfer*, Wiley & Sons, ISBN 0-471-39550-1, New York

Li, C.,H. (1986). Exact transient solutions of parallel-current transfer processes. *ASME Journal of Heat Transfer*, Vol. 108, 365-369, ISSN:0022-1481

Press, W. H.; Teukolsky, S. A., Vettering, W. T. & Flannery, B. P. (2006) *Numerical Recipes, The Art of Scientific Computing.* Second Edition, Cambridge University Press, ISBN: 0-521-43064-X, New York, USA

Roetzel, W. & Xuan, Y. (1998). *Dynamic behaviour of heat exchangers* , WIT Press/ Computational Mechanics Publications, ISBN: 1-85312-506-7, Southampton, UK.

Smith, E.,M. (1997): Thermal Design of Heat Exchanger, John Wiley & Sons, ISBN: 0-471-96566-9, Chichester, UK

Taler, D. (2002*). Theoretical and Experimental Analysis of Heat Exchangers with Extended Surfaces,* Vol. 25, Monograph 3, Polish Academy of Sciences Cracow Branch, ISBN: 83-915470-1-9, Cracow

Taler, D. & Cebula, A. (2004). Modeling of air flow and heat transfer in compact heat exchangers. *Chemical and Process Engineering*, Vol. 25, No. 4, 2331-2342, PL ISSN: 0208-6425 (in Polish)

Taler, D. (2004). Determination of heat transfer correlations for plate-fin-and-tube heat exchangers. *Heat and Mass Transfer*, Vol. 40, 809-822, ISSN: 0947-7411

Taler, D. (2005). Prediction of heat transfer correlations for compact heat exchangers. *Forschung im Ingenieurwesen* (*Engineering Research*), Vol. 69, No. 3, 137-150, ISSN 0015-7899

Taler, D. (2006a). *Dynamic response of a cross-flow tube heat exchanger*, Chemical and Process Engineering, Vol. 27, No. 3/2 , 1053-1071, PL ISSN 0208-64-25

Taler, D. (2006b). *Measurement of Pressure, Velocity and Flow Rate of Fluid*, ISBN 83-7464-037-5, AGH University of Science and Technology Press, Cracow, Poland (in Polish)

Taler, D. (2007). *Numerical and experimental analysis of transient heat transfer in compact tube-in-plate heat exchangers*, Proceedings of the XIII Conference on Heat and Mass Transfer, Koszalin-Darłówko, Vol. II, pp. 999-1008, ISBN 978-83-7365-128-9, September 2007, Publishing House of Koszalin University of Technology, Koszalin, Poland

Taler, D. (2008). Transient inverse heat transfer problem in control of plate fin and tube heat exchangers. *Archives of Thermodynamics*, Vol. 29, No. 4, 185-194, ISSN: 1231-0956

Taler, D. (2009). *Dynamics of Tube Heat Exchangers*, Monograph 193, AGH University of Science and Technology Press, ISSN 0867-6631, Cracow, Poland (in Polish)

Tan, K. S. & Spinner, I.,H. (1984). Numerical methods of solution for continuous countercurrent processes in the nonsteady state. *AIChE Journal*, Vol. 30, 770-786, ISSN: 0947-7411

Wang, C.C., Lin, Y.T. & Lee, C. (2000). An airside correlation for plain fin-and-tube heat exchangers in wet conditions. *Int. J. Heat Mass Transfer*, Vol. 43, 1869-1872, ISSN: 0017-9310

Yeoh, G. H. & Tu, J. (2010). *Computational Techniques for Multi-Phase Flows*, Elsevier-Butterworth-Heinemann, ISBN 978-0-08046-733-7, Oxford, UK

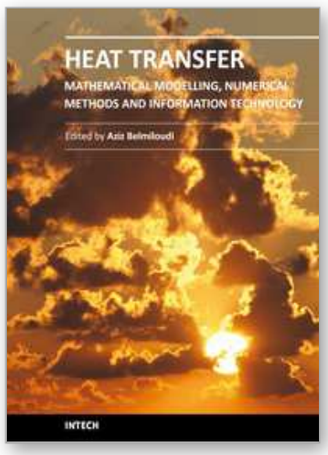

Heat Transfer - Mathematical Modelling, Numerical Methods and Information Technology

Edited by Prof. Aziz Belmiloudi

ISBN 978-953-307-550-1
Hard cover, 642 pages
Publisher InTech
Published online 14, February, 2011
Published in print edition February, 2011

Over the past few decades there has been a prolific increase in research and development in area of heat transfer, heat exchangers and their associated technologies. This book is a collection of current research in the above mentioned areas and describes modelling, numerical methods, simulation and information technology with modern ideas and methods to analyse and enhance heat transfer for single and multiphase systems. The topics considered include various basic concepts of heat transfer, the fundamental modes of heat transfer (namely conduction, convection and radiation), thermophysical properties, computational methodologies, control, stabilization and optimization problems, condensation, boiling and freezing, with many real-world problems and important modern applications. The book is divided in four sections : "Inverse, Stabilization and Optimization Problems", "Numerical Methods and Calculations", "Heat Transfer in Mini/Micro Systems", "Energy Transfer and Solid Materials", and each section discusses various issues, methods and applications in accordance with the subjects. The combination of fundamental approach with many important practical applications of current interest will make this book of interest to researchers, scientists, engineers and graduate students in many disciplines, who make use of mathematical modelling, inverse problems, implementation of recently developed numerical methods in this multidisciplinary field as well as to experimental and theoretical researchers in the field of heat and mass transfer.

InTech Europe
University Campus STeP Ri
Slavka Krautzeka 83/A
51000 Rijeka, Croatia
Phone: +385 (51) 770 447

InTech China
Unit 405, Office Block, Hotel Equatorial Shanghai
No.65, Yan An Road (West), Shanghai, 200040, China
中国上海市延安西路65号上海国际贵都大饭店办公楼405单元
Phone: +86-21-62489820

Fax: +385 (51) 686 166
www.intechopen.com

Fax: +86-21-62489821

IntechOpen